Proceedings of ICAPP '05
Seoul, KOREA, May 15-19, 2005
Paper 5081

Status of the Qualification Program of the Multiphase Flow Code MC3D

R. MEIGNEN
Institut de Radioprotection et de Sûreté Nucléaire
DPEA/SEAC
BP 17
92262 Fontenay aux Roses, FRANCE
renaud.meignen@irsn.fr

Abstract – *MC3D is a thermal-hydraulic multiphase flow code devoted to nuclear safety applications, developed by the IRSN and the CEA. It is mainly applied to the study of Fuel-Coolant-Interactions (FCI). In this paper, we provide a general presentation of MC3D, its capabilities and the status of its ongoing program of qualification. Developed since more than ten years, MC3D is now a code with very extended capabilities and functionalities. An important program of qualification has been started since two years to evaluate the initial choices for the numerical aspects, for the basic constitutive laws and to check in-depth the code capabilities. This program starts with a new evaluation of the numerical aspects (phase 0), continues with the basic 2-phase and 3-phase aspects (phase 1, underway) and finishes with the application-specific aspects (phase 2, to be started in 2006). We present the most important results of the program, and also some examples of global validation calculations for FCI and of applications to nuclear safety.*

I. INTRODUCTION

MC3D is a software devoted to multiphase flows studies and evaluations in the field of nuclear safety. Developed since more than ten years, its field of applications has evolved several times to become one of the reference tools for the evaluation of Fuel Coolant Interaction. In particular, it is used by IRSN, CEA and partly IKE in the frame of the OECD program SERENA[1]. It is currently used for evaluations of ex-vessel[4] and in-vessel FCI's in the frame of a PSA level 2, thus attesting its potentials and the robustness. To do this, the code has been qualified versus the most important FCI experiments (FARO[2] and KROTOS[3] in particular).

In parallel, an ambitious and in-depth program of qualification has been started, covering several aspects from the basic numerical features to FCI specific models. The program is separated in 3 distinct phases. Phase 0 concerns the numerical aspects, phase 1 investigates the basic 2-phase and 3-phase models, whereas phase 2 is devoted to FCI-specific features. The program will be accomplished with an evaluation of the main specific modellings that cannot be easily confronted to analytical or experimental data, such as the flow map or heat and mass transfer mechanisms under the shock-induced fragmentation of a fuel drop. Phase 0 and 1 are now mostly achieved and we will give here the most representative results.

The last part of the present paper will be devoted to the general qualification of the code relatively to the current applications. This concerns of course the FCI but also the evaluation of the Direct Containment Heating phenomenon. For the latter, as we are on the beginning with this work, we mainly pay attention to the dynamical aspects, thanks to the elaborate handling of the fuel flow. Beside the interest for the DCH phenomenon itself, the confrontation of MC3D with DCH experiments gives some further insight of the capabilities of the main models of the code.

II. GENERAL PRESENTATION OF MC3D

Some presentations of MC3D can be found in the literature. They are however quite old. The first description of the FCI premixing models is due to Berthoud and Valette[5]. Since then, the code has been largely improved. Some insight of the code can also be found in a paper describing its use in calculations of flashing propane jets[6].

The purpose of MC3D is to study multiphase and multi-constituent flows. It is developed in a modular way with a so-called concept of "application". An application, in the sense of MC3D, is simply a set of mass components, momentum and energy mixtures, coupled through constitutive laws. All applications are built under the same structure and use the same mathematical model and resolution core. Due to the flexible structure of MC3D, about 10 different applications have been built in the past for different purposes. However, if building an application can be rather easy (provided you have the adequate modeling) maintaining it can be quite heavy if it is no more used. Indeed, only 3 of these applications have been maintained:

- FCI premixing;
- FCI explosion;
- 2-phase flow with heat and mass transfer in porous media.

The latter application is in fact not directly included in MC3D but has been separated from the code in an autonomous software. It has however exactly the same structure.

The premixing application is a very complex model that in fact allows the use of the code for other purposes, such as DCH. This is also the reason why we did not maintain simpler applications which where in fact included in the premixing one.

II.A. Mathematical model

Each application contains its own set of mass, momentum and energy balances, but they all use the same mathematical model and resolution core. The number of equations of mass, energy and momentum is variable from one application to another. Phase transfers can be taken into account by mass transfers between components (evaporation, condensation or simply fragmentation/ coalescence). The mechanical coupling between components is ensured by the pressure, interfacial frictions and the possible mass transfers between components. The thermal coupling between the mixtures is ensured by heat and mass exchanges between mixtures.

Balances are written in an Eulerian way on a structured mesh with cartesian or cylindrical geometry. For the resolution we use the standard ICE method:

- Use of the momentum balances to express velocities according to the local and neighboring pressures.
- Integration of this expression in the energy and mass balance.
- Combination of the equations to obtain a pressure system.
- Resolution of this system by a linearization with an iterative Newton-Raphson type method.

This method has the advantage to be fast and robust. It allows a semi-implicit treatment, necessary because of the strong mass transfers. On the other hand, it presents the disadvantage of not being very evolutionary.

The main variables are the volume and mass fractions, velocities, the (single) pressure, and the temperature (with the exception of the explosion application where the enthalpy is the thermal variable)

Mass and energy balances are written in a Finite Volume form. Momentum balances are expressed with finite differences and a quite standard non-conservative form. Due to the importance of the convective aspects in premixing, we will give later some details on the momentum balance.

Beside these general trends, each application can have its proper particularities as the fuel volume tracking method and the interfacial area transport equation in the premixing.

II.B. Overview of FCI applications

The MC3D premixing model is a 6-field application in which the melt is described by 3 fields (Figure 1). The fist one is called "continuous" and can describe many situations as, for example, a jet or to the melt lying on the bottom of a vessel. The second field corresponds to the droplets issued from the jet fragmentation. This field describes necessarily a discontinuous state of the fuel. The third field is optional and describes the fuel fragments issuing from drop fine fragmentation. The remaining three fields are the water, the vapor and one non-condensable gas. Note that in the next version (3.5), several non-condensable gases will be available.

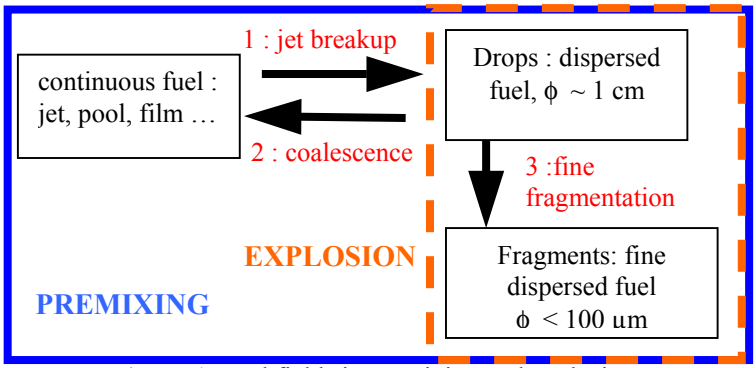

Figure 1: Fuel fields in premixing and explosion applications

Drop surface area is modeled with a standard Ishii-like interfacial area transport equation. Alternatively, drops can be replaced by solid balls with a specified diameter. In that case, the continuous fuel field is also not considered.

In the explosion model, the continuous phase is not present and only the two fields related to dispersed fuel are

considered. There is however a second difference between the two applications in that in the premixing tool, the fuel fragments are in equilibrium with the water. For the explosion, the fragments have their own dynamical and thermal fields. They interact with the coolant in a similar way to the drops; in particular, the coolant mass transfer that they impose is calculated thanks to a desequilibrium approach.

All fields are treated in an eulerian way, but the continuous phase is the object of a special treatment, with a VOF-SLIC method. This method allows for a good tracking of the fuel interface and suppresses all numerical diffusion.

The major features of the physical models and constitutive laws are described in a separate paper together with those of the codes participating to SERENA[7]. It is thus not necessary to details them here. We will only describe the continuous fuel field model and the flow map.

II.C. About fuel treatment in premixing

One of the most important particularities of MC3D is the fact that, in premixing, the fuel is described by two fields (optionally three if we use the fragments). These two fields describe the two possible states of the fuel: either continuous, either discontinuous. In contrast with most of the either eulerian codes, the distinction is not based on geometrical arguments (the volume fraction) but is ensured by two specific fields, connected by mass transfers (fragmentation or coalescence, Figure 2). This way, the drop field is supposed to describe only discontinuous fuel drops.

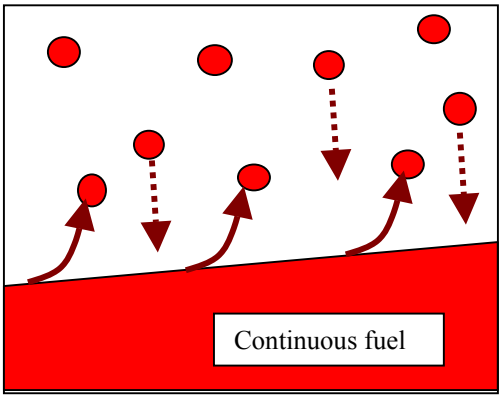

Figure 2: Connections between the continuous and discontinuous fuel fields. Plain arrows: fragmentation; dashed arrows: coalescence towards continuous fuel.

The fragmentation process is obtained either through a correlation[8,7] either a local model taking into account local velocities[7]. Coalescence occurs either from drop collision with the continuous fuel, either from collision between drops. In both cases, the collision models are simple and mostly based on geometrical arguments. When the drops are in a solidified state and coalescence is impossible (or in case of solid balls), a model implementing the effect of elastic collision is used, in order to ensure a sufficient dispersion. This way, solid debris beds can be considered.

The continuous fuel is modeled with a VOF-SLIC method. It is however available only in 2-D geometry. In this method, the continuous field is supposed to be bounded by a linear interface in each cell (Figure 3). The two parameters to be determined for each cell are the normal vector $\vec{n}$, and height of the interface (B_Z). The normal vector is obtained by inspection of the surrounding cells and assuming the functional form:

$$\alpha_c = ax + by + c$$

where α_c is the continuous fuel volume fraction. $a = \frac{\partial \alpha_c}{\partial x}$ and $b = \frac{\partial \alpha_c}{\partial y}$ are the coordinates of the normal vector, and are calculated by a least square method considering the 8 surrounding cells and the local one. Among the different tested methods, this one gave the best representation with distorted cells (i.e. one side far larger than the other). B_Z is obtained by simple geometric arguments. In this model, the convection of the fluid is calculated according the effective common area of the fluid with the cell boundary. This is illustrated in Figure 4, where the dashed areas represent, for a case of two fluids, the amount of fluid convected during the time step dt. With the configuration depicted in Figure 3, no fluid is convected towards the right and the top of the cell.

A simple illustration of the capabilities of the method is shown in Figure 5 depicting two Rayleigh-Taylor flows (2-fluid mixing by gravity, heavy fluid on top) with two different meshes.

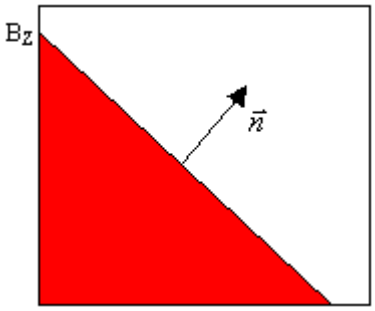

Figure 3: Picture of the VOF-SLIC method

Figure 4: Convected volume with the VOF-SLIC method: red = tracked fluid.

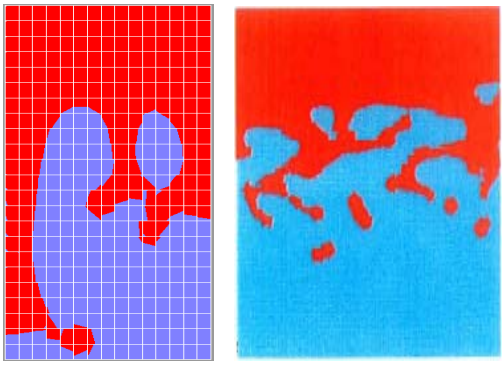

Figure 5: Illustration of the VOF-SLIC method with 2 Rayleigh-Taylor flows (red = heavy fluid) with coarse and fine meshes.

II.D. The flow map

Concerning the other fluids, the flow characteristics, and the resulting interaction laws are described according to a flow map based on the volume fraction of the liquid coolant and the gas (Figure 6). In all cases, we consider that the flow is a composition of a bubbly zone and a droplet zone. Denoting F_B and F_D the volume fractions of the bubbly and droplet zone, and α_B and α_D some regime bounds relatively to the void fraction α:

- if $\alpha < \alpha_B$: bubbly flow, liquid coolant is continuous and all fuel drops are in contact with water (in film boiling), $F_B = 1$, $F_D = 0$;
- if $\alpha > \alpha_D$: droplet flow, gas is continuous with liquid droplets. Fuel drops are considered in contact with the gas, $F_B = 0$, $F_D = 1$;

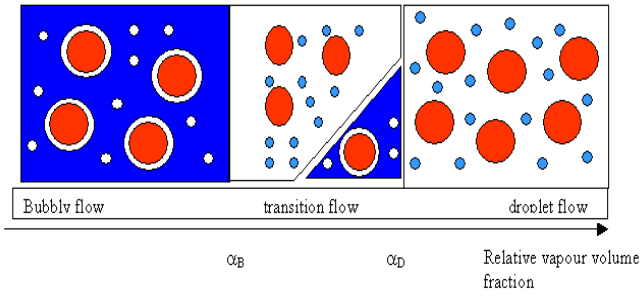

Figure 6 Representation of the flow map in MC3D

In between is the transitional flow. Considering the representation in Figure 6, F_B (resp. F_D) is the volume fraction of the white zone (resp. blue zone) , including the fuel drops and the coolant droplets (resp. bubbles and vapor film). The sum of F_B and F_D always equals to 1. F_B and F_D are calculated such that the bubble volume fraction relatively to the bubbly zone is α_B and the droplet volume fraction relatively to the droplet zone is $(1- \alpha_D)$. Then the regime bounds have finally two meanings: they determine the flow pattern transitions and give the maximum bubble and droplet volume fractions. With this concept, we can describe various kinds of flow, including purely continuous flows with no inclusion ($\alpha_B = 0$, $\alpha_D = 1$), purely mist flow ($\alpha_B = 0$, $\alpha_D \Rightarrow 0$), or foams ($\alpha_B \Rightarrow 1$, $\alpha_D = 1$). The fuel drops and fragments are uniformly distributed in the mesh, and thus proportionally to F_B and F_D. There is no physical justification to this choice. This way, the effective flow bounds have a third influence if, as in FCI, the fuel drops mostly interacts with one of the coolant phase. In FCI, increasing α_B, will also increase the fuel volume fraction in effective contact with water. The overall effect and qualification of this choice of representation is still not very clear and will be the object of work in the near future. A complementary discussion on this point can be found in ref.7.

The standard value of the regime bounds α_B and α_D are 0.3 and 0.7. Note that for the explosion, the fragments behave in the same manner as the drops. The flow map is very important in MC3D because all constitutive laws are based on the same scheme. All laws (friction, heat transfer, mass transfer) are calculated by considering the two separate bubbly and droplet regime, and simply adding the two contributions. As an example, consider the fuel drop skin friction with water F_{dl}:

$$F_{dl} = F_B.F_{dl,bubbly} + F_D.F_{dl,droplet} \quad (1)$$

III. MAIN RESULTS OF THE QUALIFICATION PROGRAM

The qualification program is superposed to the standard validation tests accompanying each evolution. It is intended to give a precise knowledge of the validity of the various numerical models and constitutive laws introduced in MC3D. Due to the high number of such laws and models, it is not possible to track in detail the results for each one. The objective is then first to verify that the basic laws calculated by the code are consistent with what is supposed to be in. Second, we seek to evaluate the validity of the choices made by comparison with analytical models or experiments. Future developments will be chosen according to the results of this program. Up to now, the basic models that have been extensively verified are:

- the convection of fluids
- the continuous field volume tracking method
- the pressure wave/shock propagation
- the 2-phase friction for fuel drops, bubbles and liquid drops
- the solid ball and drop fragmentation in gas flow
- drop heat transfer in single phase flow

Among the various tests, only the results concerning the convection, the shock propagation and the solid ball frictions will be illustrated here. As already explained, specific features with multi-fluid systems will be considered in the next phase of the program.

III.A. Convection scheme

Since version 3.4, a new convection scheme is available. The previous scheme was written in a quite standard upstream finite difference non-conservative manner. This one led to some difficulties in the convection of dispersed phases. It has been corrected with an original scheme written in a conservative finite volume way. For a given face, the velocity is calculated with a finite volume mass balance over the two adjacent cells. In a 1-D formulation, this leads to (Figure 7):

$$\frac{\alpha\rho\Delta U_i}{\Delta t}+\frac{\langle\alpha\rho U\rangle_{j+1}\Delta x_i+\langle\alpha\rho U\rangle_{j-1}\Delta x_{i-1}}{\Delta X_i}\frac{\Delta U_i}{\Delta x}=0 \quad (2)$$

The scheme is then centered and it is well known that instabilities are to be expected. These ones are avoided thanks to a detection of unstable situations (analog to the CFL condition) and smoothly switching to the standard upstream scheme when necessary. When coupled with a second order model for the calculation of the convected volume fractions (the α's in the bracket of (2)), this leads to a very satisfying scheme, essentially of second order.

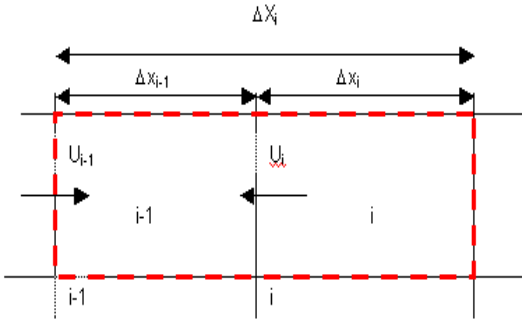

Figure 7: 1-D representation of the grid attached to the new convection scheme.

The results with this scheme are illustrated with the 1-d standard problem of convection of a dispersed fuel field. We consider here the convection of drops with volume fraction of 10 %, and initial velocity of 5 m/s. Inside the computational domain, the fuel drop volume fraction is residual (10^{-5}) and the velocity is zero. Skin frictions are minimized. The grid is representative of reactor scales with a length of 5 m for 30 cells. The results are given in Figure 8 where we show the drop volume fractions and velocities at different locations. The propagation is very accurate and no oscillatory behavior is obtained.

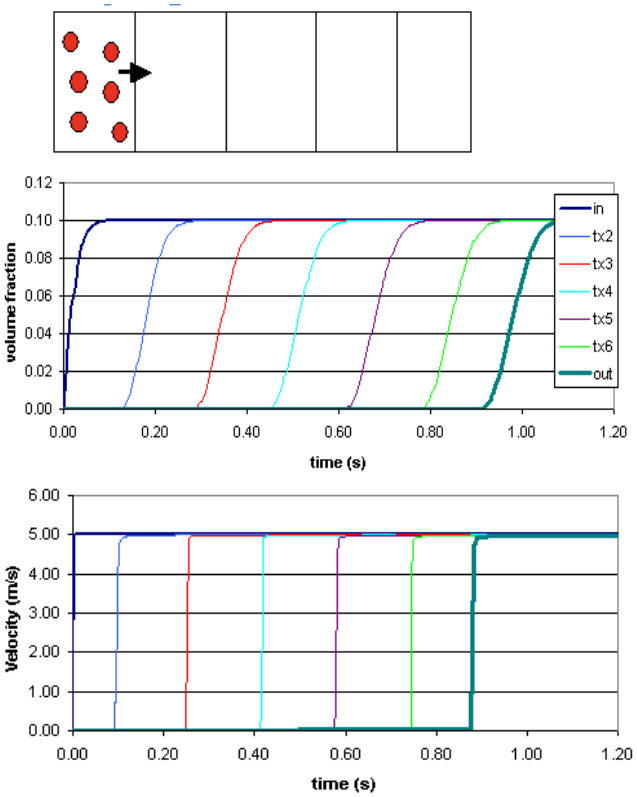

Figure 8: Results of the 1-D drop convection test with reduced skin frictions: drop volume fractions and velocities with time at several locations.

III.B. Pressure wave propagation

Still in the domain of numerics, we illustrate now the behaviour of the codes relatively the wave propagation. For MC3D, which is mainly used for FCI, this is obviously an important task. Figure 9 gives the result of the calculation of the KROTOS test KT4 that is a test of the propagation of the trigger pulse in pure water. Each graph corresponds to a location along the test section, K0 being at the trigger position and K5 being near the water level. We see that the propagation and reflection of the wave is perfectly calculated, except a little delay. This is only due to the sound velocity that is not exactly the theoretical one in the experiment (1530 ms^{-1} calculated versus 1300 ms^{-1} in the experiment).

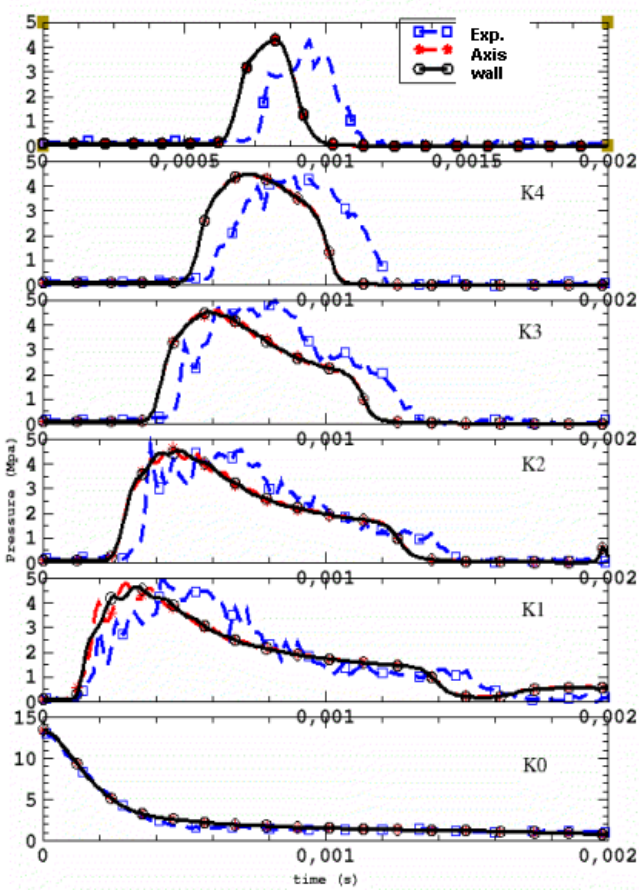

Figure 9: Propagation of the pressure wave in the test KROTOS KT4, at different positions along the test section

Figure 10 illustrates the results of calculations of shock waves in water-gas 2-phase flows. The initial conditions are given in each graph with a thin dashed line. Initially, the domain is separated in two regions with, on the left, 20 bar, 50 % void and a gas temperature of 500 K, and on the right, 1 bar, 4 % void and 700 K respectively. No heat and mass transfer is considered and we use standard parameters. The grid is here also characteristic of reactor conditions. The calculation is compared with an analytical resolution and a fully satisfying behavior is obtained.

III.B. Particles skin frictions

Coming now to the constitutive laws, we will address here the case of skin frictions of drops and bubbles in purely 2-phase flow.

For the frictions relative to the drops or solid balls, we use the two different laws, according to the particle volume fraction. For dilute to moderate volume fractions (30 %), we use the laws derived by Ishii[9,10]. For multiphase flows, these laws have been extended, using the same mathematical model as Ishii. In the case of dense flows (α > 40 %), we use either the classical Ergun law[11], either the Gibilaro correlation[12]. The transition is ensured by a simple interpolation between the two regimes. In the present calculations, we consider flows of solid balls with characteristics close to those for the reactor case. The cases considered for the study are those in the experiments of Richardson & Zaki[13].

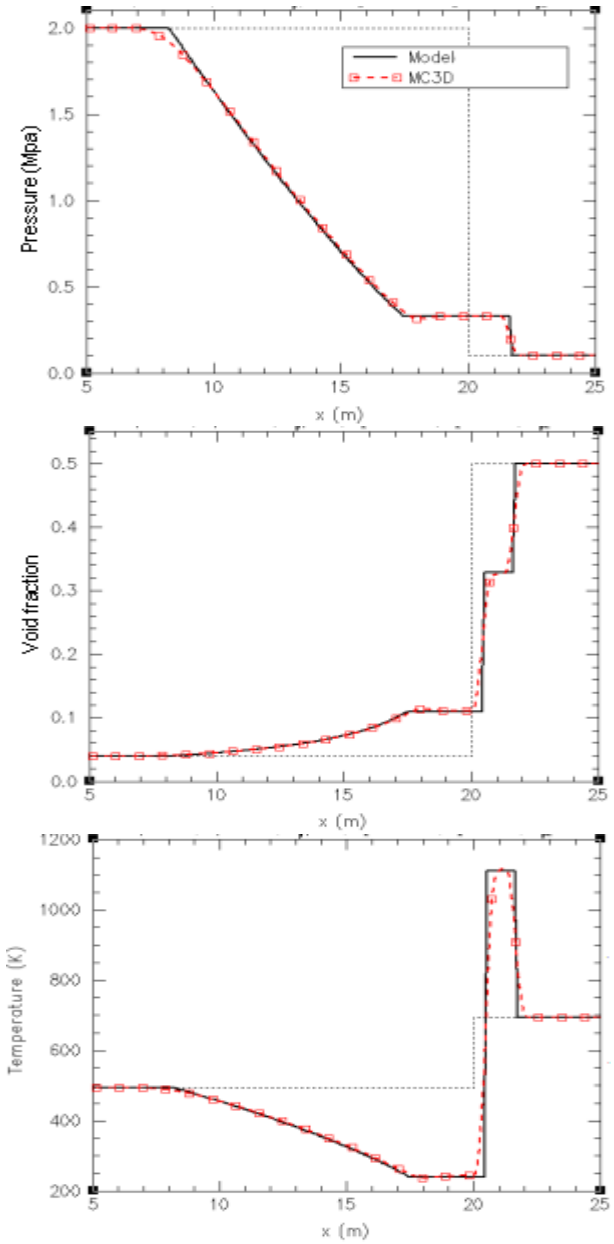

Figure 10: Results for the pressure, void fraction and temperature in the propagation test in 2 phase bubbly flow; dashed line = initial state: left side: α=0.5, P = 2Mpa, T = 500 K, right side : α=0.04, P = 0.1 Mpa, T = 700 K

We find that the use of the famous Ergun law is really correct only for very dense flows, and is finally not very

suited for balls of the order of some millimetres. Indeed, the use of the Ishii's laws in conjunction with the Gibilaro correlation gives better results for most of the cases (Figure 11). The case of the viscous regime does not show these differences for the dense flow. In fact, in all cases, we find that the Ishii's law is still correct for the dilute to moderate flows but the dense regime shows noticeable discrepancies with the model of Richardson & Zaki (Figure 12). However, this case is not so critical as dense flows in the viscous regime are not important in the applications considered with MC3D.

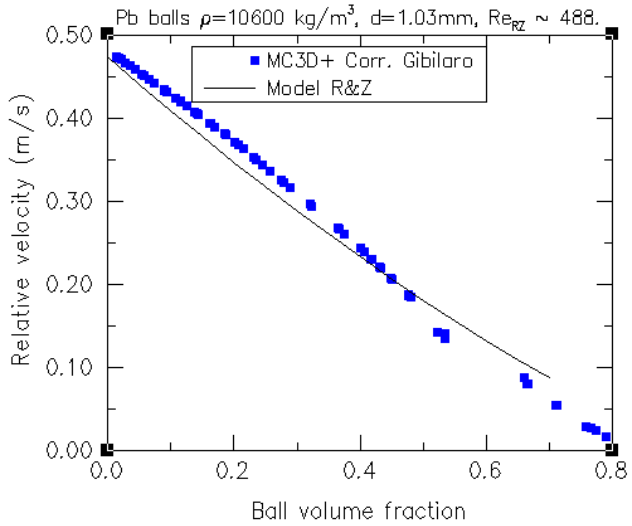

Figure 11: Comparison of the velocities in a flow of solid balls, in the Newton regime (premixing), as compared to the model of Richardson & Zaki, with the use of Gibilaro correlation law for dense flows.

A similar study was performed for purely bubbly flows, with comparison of the rising velocity with the Ishii model[9], and data compiled by Wallis[14] (pure non contaminated water) and Clift et al.[15] (industrial water). Following Ishii, results are expressed in dimensionless variables for the velocity and equivalent radius:

$$v^* = v_\infty \left(\rho_c^2 / \mu_c g(\rho_c - \rho_b)\right)^{1/3} \quad (3)$$

$$Rb^* = R\left(\rho_c g(\rho_c - \rho_b) / \mu_c^2\right)^{1/3} \quad (4)$$

and shown in Figure 13 for two different volume fractions. The agreement with data of Clift (industrial water) is far sufficient.

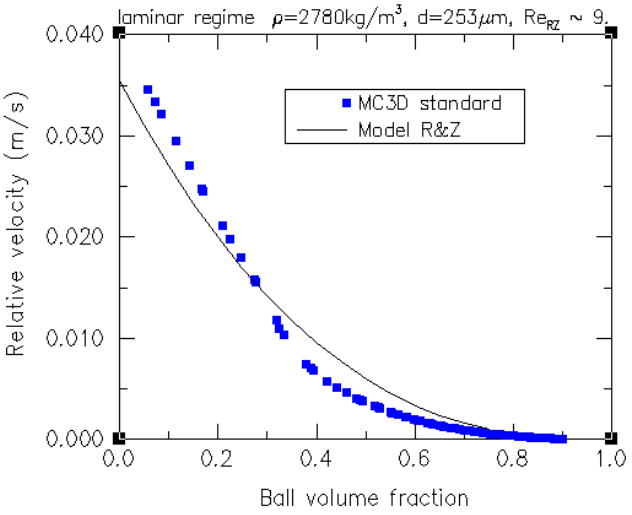

Figure 12: Comparison of the velocities in a flow of solid balls, in the viscous regime (small particles), as compared to the model of Richardson & Zaki

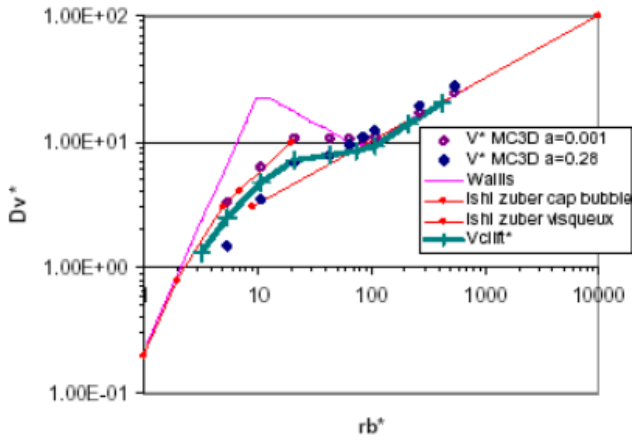

Figure 13: Comparison of calculated velocities with the models of Ishii and data from Wallis and Clift for two different bubble volume fractions (0.1 % and 28 %).

IV. COMPARISONS WITH MORE GLOBAL EXPERIMENTS

At an intermediate level of complexity between analytical tests and FCI experiments, MC3D has also been compared to various experiments concerned with multiphase flows. We will here focus on experiments involving dynamical aspects.

IV.A. Cold solid ball jets

Among these tests, the calculation of jets of cold balls as in BILLEAU test is regularly performed. Figure 14 shows the result of a calculation of the BILLEAU FPV12 cold test[16]. This test involves a plane jet of solid glass balls

(ϕ = 10 mm) in cold water. Results are given in Figure 14 for the penetration depth and Figure 15 for a visual comparison of the flow.

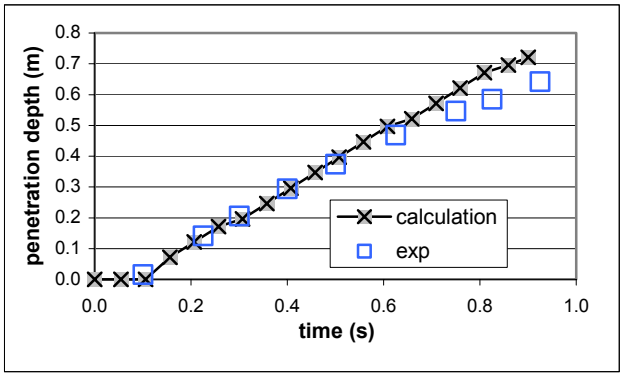

Figure 14 Penetration depth of the ball jet in a BILLEAU FPV12 test calculation.

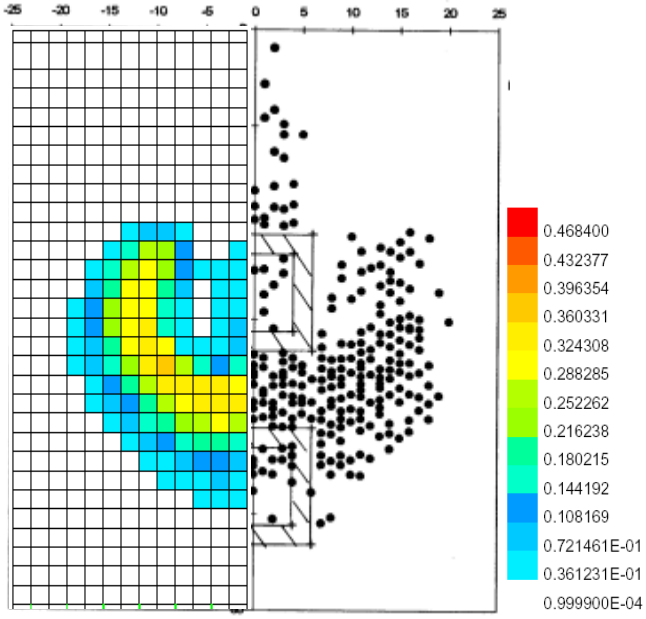

Figure 15 Visual comparison of the ball distribution in BILLEAU FPV12 test calculation at t = 0.7 s. (calculated volume fraction on left, ball positions on right)

IV.A. Melt ejection from a pressurized vessel

MC3D is also currently extensively tested for DCH applications. This complicated process involves several features, the first of which is the melt ejection from the vessel. This feature is of course of interest also in FCI studies for the reactor ex-vessel case. Recent experiments, named DISCO, have been performed at FZK with the EPR geometry at reduced scale (~1/16) with cold simulants[17]. Of particular interest is the case where the simulant is a metal. In the test M02, the vessel contains 29.5 kg of Wood's metal, is pressurized at 6 bar and the breach diameter is 25 mm. A visualization of the flow at the breach is proposed in Figure 16. Figure 17 compares the calculation of the pressure in the vessel and the depressurization rate with the experimental ones. The discrepancies with the experiment are seen to be of second order. The transition towards the two-phase flow at the breach occurs approximately 10 ms before the experiment, but this has no influence on the overall process. Only a limited sequence of the depressurization rate in inadequately computed, with here also very limited consequences. Once a transition form single-phase to two-phase flow has occurred at the breach, the simulation of such phenomenon is not so obvious. The results indicate a good opening process of the gas flow area, and thus probably a satisfactory general computation of the fuel flow pattern.

New similar experiments are currently performed at FZK with a geometry representative of the French PWR reactors[18]. In the cold test series, experiment F07 involves a flow of water with breach diameter of 60 mm and a vessel pressure of 16 bar. A visualization of the initial conditions and of the flow at two different times is given in Figure 18. The results concerning the pressure inside the vessel and in the cavity at the point of impact is provided in Figure 19. Due to a lower density, the liquid ejection patterns are different form the previous case. Here also, a very reasonable accuracy is obtained. The resulting dispersion of the liquid in the cavity and the two outlets (to containment and compartment) is also well computed.

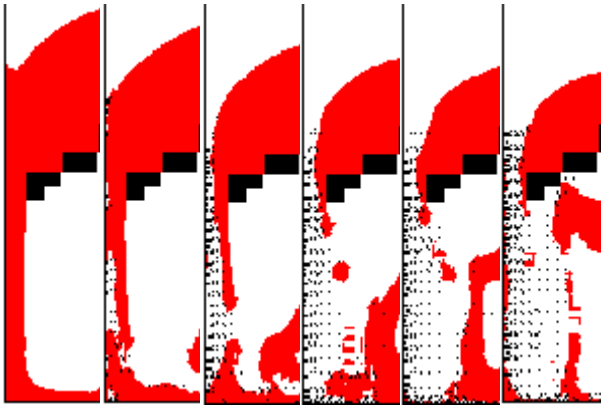

Figure 16 Visualization of the flow at the breach in the calculation of DISCO M02, at the time of two-phase flow transition: blue : continuous fuel field, black dot : fuel drops

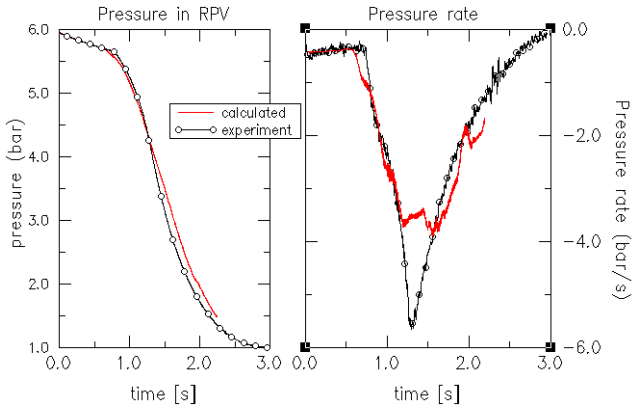

Figure 17 Calculation of DISCO M02 test with Wood's metal: pressure inside the vessel and depressurization rate.

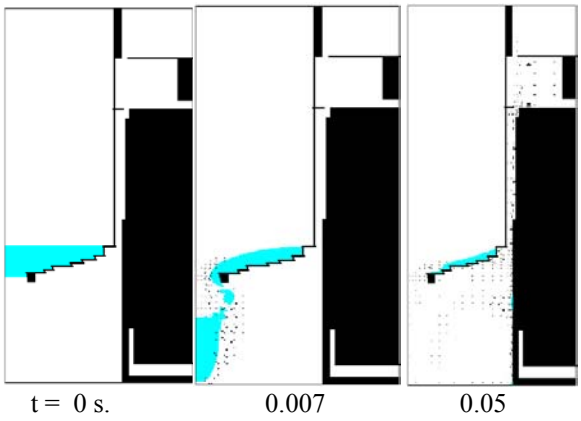

Figure 18: Visualization of the fuel flow pattern DISCO F07, blue : continuous fuel field, black dots : fuel drops.

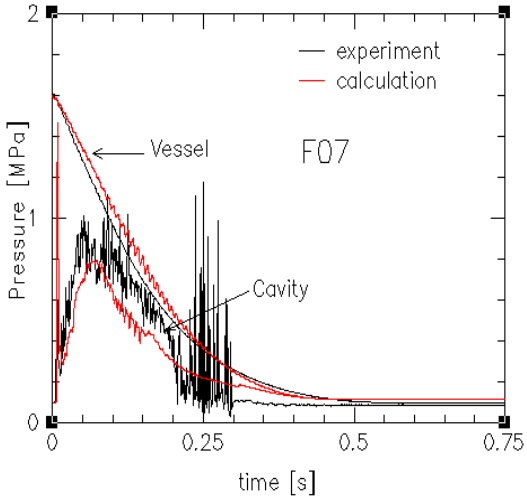

Figure 19: Calculated and experimental pressures in the vessel and in the cavity for test F07

V. STATUS OF QUALIFICATION FOR FCI

The current status of qualification of the code has been partly given in the frame of SERENA. For this particular purpose, calculations where performed with the standard parameters of the code, i.e. those that are supposed to be the most adequate from the physical point of view. In parallel a second qualification process was done in the frame of a PSA level 2 study of FCI potential in both in-vessel and ex-vessel situations. With the help of these two different works, it is possible to clarify the degree of qualification and the needs for improvements.

V.A. Status of qualification for the FCI premixing

Calculations for SERENA task-2 and 3 where performed with the underlining idea of checking the various models with what is supposed to be the most adequate set of parameters. For the PSA2 calculations, the parameters where adjusted in order, first to provide the best fit to the FARO experiments and second to minimize the various imperfections obtained with the standard models. The results with these parameters have already been exposed elsewhere and we will thus here only analyse the meanings of these differences. This will give a quite clear perspective of the various needs of modelling. The differences between the two methods are given in Table 1.

The most important difference is relative to the jet fragmentation. Some insight of the models can be found in reference 7. In Task-2, a correlation deduced from a complex instability model was used. The correlation does not provide a size for created drops, thus a constant parametric value is used. This correlation was specifically build and fitted for FARO-like jets. The suitability in different conditions is not ensured, as for all other laws used in other codes since, today, FARO is nearly the unique reference for premixing using prototypical materials and high fuel masses. This is why we also built a model using local conditions, based on an extension of the Kelvin-Helmholtz model to multiphase flows. Both models give good results for FARO jets, whatever the conditions. Differences are obtained only on the diameter of the drops, where the local model gives generally slightly smaller drops. However, when extrapolations to different conditions are done (reactor situations, see Task-4 results[19]) really important differences are obtained. Presently, it is not possible to know which model is the most reliable. This enlightens the real need for experimental premixing data with different conditions than in FARO (water height, fuel pouring process).

Model / Parameter	Task 2 Values	PSA level 2 values
Jet fragmentation model	Meignen correlation 2 diameter for created fuel drops = 4 mm	Local model based on Kelvin-Helmholtz model. => drop diameter calculated d = 0.2 λ
Bounds in the flow map: α_B, α_D	0.3 – 0.7	0.4 – 0.6
Bubble critical Weber number	12	Based on the correlation of Yoneda for the bubble mean Sauter diameter.
Correction of convective fuel to gas heat transfer	1.	0.3

Table 1 : Parameters and models modified between the SERENA task-2 calculations and the PSA2 qualification process.

More important in view of qualification versus experiments are the modification of the bounds in the flow map (see section II.B) and the bubble stable size model. These are related to the quite general tendencies of most of the codes to lead to too much void without necessarily having sufficient pressurization. The use of different bubble critical Weber number, based on the Yoneda experiments[20], is particularly important in this respect. Further clarifications and qualifications are needed on this point.

A more puzzling point is the strong decrease of the fuel to gas heat transfer that seemed necessary to reduce the gas temperature in accordance with most of the premixing experiments. The heat convection model has been qualified in a satisfactory way and it is thus difficult to understand the reason of this need for such a strong decrease need.

Other modifications are of secondary importance and are more related to numerical improvement than real modelling issues.

Thus concerning premixing, it seems that the really important work done in this area has led to a quite satisfying status, where further improvements seems to be reachable in a quite near future. For the coolant flow map and related processes, it is likely that an in-depth qualification would help to clarify the problem. Concerning the fuel fragmentation, the problem is trickier and we will probably need some further experiments involving various geometries.

V.B. Status of qualification for the FCI explosion stage

FCI modeling has started with global thermodynamically models, then has proceed with more complex detonation models. Although they are really worth for understanding the basics of the explosion process, these models could not achieve a satisfying state that could give sufficiently relevant estimates of the pressure loads. It then appeared that the problem would not be handled in a relevant manner without paying strong attention to the premixing process. It seems that since then most of the work on FCI focused on this stage. Looking precisely at most of models for the explosion stage[7], we find that explosion models have not strongly been improved since a quite long time[*]. As it seems that premixing models are on a rather good way, it is probably time to pay more attention on the explosion processes i.e. the fine fragmentation and the heat and mass transfer process.

In MC3D, the explosion is treated in a quite similar manner as the premixing, with however different assumptions on the constitutive laws. These laws are similar to those used in other codes participating to SERENA. Thus it is quite likely that a general lack of knowledge and understanding exists. As for other codes, the model has been firstly checked and fitted versus KROTOS experiments. We can then say that the global picture of the process is satisfactory. However, SERENA task-3 has revealed some weaknesses, particularly with the calculations of experiments with corium. It seems that, in comparison with the alumina test calculations, an important reduction of the heat transfer (whatever the mean: fragmentation, melt area, heat transfer process of coefficient) was necessary, even if the order of magnitudes are correct.

As an illustration, we can investigate the effect of one of the weaknesses of MC3D: the constant parametric value of the diameter of the fragments. This lack is common to all codes used in SERENA. Figure 20 gives the results of calculations of FARO L-33 when we vary the diameter from 100 to 400 µm. The calculation is done in two separate phases with the premixing and then the explosion. Whit the most recent version of the code, the premixing is calculated still with the parameters established for the PSA2 study. We obtain approximately the same results as those given in reference 4. For the explosion calculations, we use the standard parameters except for the fragment diameter that is used as the sensitivity parameter. The standard value in the code is 100 µm, i.e. the approximate value of fragment size in KROTOS-alumina experiments[3]. In the code, the explosion is triggered at the same time as in the experiment. We find that an important over-estimation of the loads is obtained with the standard value for the fragment diameter, as it was concluded from

[*] There is however an exception with the process of thermal fragmentation where an important experimental and theoretical work has been done. However, strong uncertainty still persists on this subject.

SERENA task-3. Note however that the order of magnitude is relatively correct, especially in the upper part of the test section. Diameters of 200 µ give relatively satisfactory results on the mean for both the amplitude and propagation of the pressure. However, there is a second strong peak of pressure that is not explained. It is seen that the sensitivity of the fragment diameter is very important. With 400 µm, nearly no explosion is obtained. Obviously, if fragmentation results from hydrodynamic processes, there is no reason why the average diameter should always be the same. For the case of interactions with corium, we do not have sufficiently precise debris distribution. However, data from TROI experiments[21] tends to show that an average value around 400 µ might be more indicative than 100 µm.

It is clear that, although calculations might be correct at first order, there is a need for further investigation of the various processes involved in the explosion.

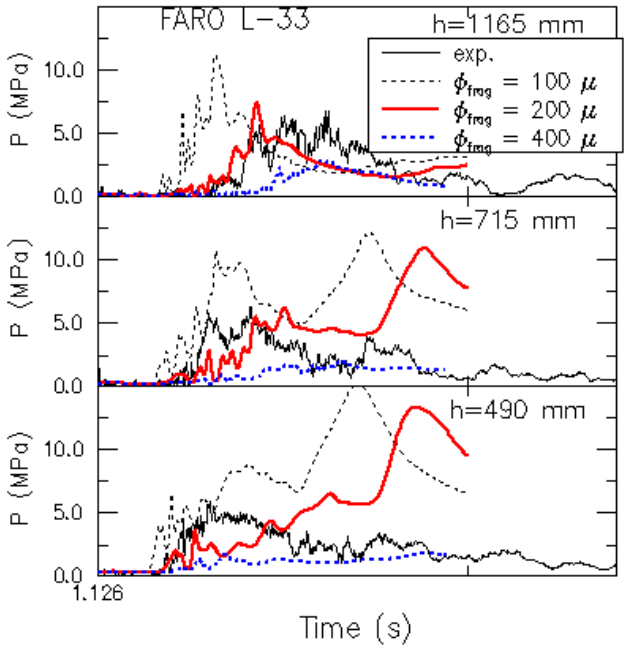

Figure 20: Sensitivity of the fragment diameter in calculations of FARO L-33. Each graph corresponds to the pressure at the prescribed height of the test section.

VI. CONCLUSIONS

After more than ten years of development, the multiphase flow code MC3D has attained a high level of functionality and reasonable validation versus FCI experiments. However, due to the complexity of the code, it was necessary to check in depth the qualification of the most important models and laws introduced in the code. We have presented a summary of the status of this qualification process. Currently, only the basic models have been checked and corrected when necessary. Once this first phase of the qualification program is achieved, we will be able to focus on less trivial features regarding to the FCI specific models and their extrapolation in multiphase flow environment. It is however clear that there is some needs of clarifications for various points, and particularly for all processes for fuel fragmentation during both the premixing and the explosion. These clarifications won't probably be obtained without supplementary experiments.

ACKNOWLEDGMENTS

This qualification program is jointly performed with the CEA in the frame of a collaboration program on FCI.

NOMENCLATURE

α volume fraction (void if no subscript)
α_B bounding void fraction between bubbly and transitional flow, also bubble volume fraction in bubbly zone.
α_D bounding void fraction between droplet and transitional flow, 1 - α_D is also the droplet volume fraction in droplet zone.
d diameter
F_B bubbly zone volume fraction
F_D droplet zone volume fraction
F_{dl} skin friction between fuel drops and liquid coolant
g gravity
λ wavelength of instability
R radius
v velocity
ρ density
μ viscosity

Subscripts:

b bubble
d drop
c continuous or coolant
j jet
g gas
l liquid

REFERENCES

1. D. Magallon et al. "OECD Programme SERENA : Work Program and First Results. ". *Nureth 10, paper G00107,* Seoul, Korea, (2003)
2. D. Magallon and I. Huhtiniemi, "Corium melt quenching tests at low pressure and subcooled water in FARO", *Nuclear Engineering and Design*, **Volume 204, Issues 1-3**, Pages 369-376 (2001)

3. I Huhtiniemi, H. Hohmann, D. Magallon, "FCI experiments in the corium/water system", *Nuclear Eng. Design*, **vol 177**, 339-349, (2002)
4. First Evaluation of Ex-Vessel Fuel Coolant Interaction with MC3D", *Nureth 10, paper G00306*, Seoul, Korea, (2003)
5. G. Berthoud and M. Valette, "Development of a Multidimensional Model for the Premixing Phase of the Fuel Coolant Interaction", *Nuclear Engineering and Design*, **Volume 149, issue 1-3**, p.409-418 (1994).
6. Simone Vandroux-Koenig and G. Berthoud, "Modelling of Two-Phase Momentum jet close to the breach, in the containment vessel of a liquefied gas*", J. of Loss Prevention in the Process Industries*, **Volume 10, Issue 1**, p. 17-29 (1997)
7. R. Meignen, D. Magallon et al., " Comparative review of FCI Computer Models Used in the OECD-SERENA program", *ICAPP-05*, Seoul, South Korea, Paper 5087 (2005)
8. R. Meignen, "Modélisation de la Fragmentation d'un Jet Liquide à Très Haute Température dans un Liquide Froid Volatil*", Ph.D. thesis, INP Grenoble*, France (1995)
9. M. Ishii, N. Zuber, "Drag coefficient and relative velocity in bubbly, droplet and particles flows", AIChE J. 25 p.843-855, (1979)
10. M. Ishii, K. Mishima," Two-fluid model and hydrodynamic constitutive relations", *Nuclear Eng. and Design*, **82,** p.107-126,(1984)
11. R. K. Niven, "Physical insight into the Ergun and Wen & Yu equations for fluid flow in packed and fluidized beds", *Chem. Eng. Sci.*, **57**, p.527-534, (2002)
12. H. Enwald, E. Peirano, A.E. Almstedt*, "*Eulerian two-phase flow theory applied to fluidization*", Int. J. Multiphase Flow*, **Vol.22, Suppl**., pp. 21-66, (1996).
13. J.F. Richardson, W.N. Zaki," Sedimentation and fluidization : part I", *Trans. Instn Chem. Engrs*, **vol. 32**, (1954).
14. G. Wallis, "One-dimensinal two-phase flow", Mac Graw-Hill, (1969)
15. R. Clift, JR Grace, ME Weber, "Bubbles, drops and particles", *Academic Press*, (1978)
16. T. Oulman, M. Hamon, "Rapport d'essai BILLEAU FROID essai FPV12", NT STR/LTEM/96/17, (1996)
17. L. Meyer., M. Gargallo," Low Pressure Corium Dispersion Experiments with Simulant Fluids in a Scaled Annular Cavity", *Nuclear Technology*, **141**, pp.257-274 (2003)
18. R. Meignen, C. Caroli, D. Plassart, L. Meyer, D. Wilhelm, " Direct Containment Heating at low primary pressure: experimental investigation and multidimensional modeling", to be presented in *Nureth11*, Avignon, France, paper 164, (2005)
19. D. Magallon et al. " Status of international programme SERENA on fuel-coolant interaction", *ICAPP2005,* paper 5382, Seoul Korea (2005)
20. K. Yoneda, A. Yasuo, T. Okawa "Flow structure and bubble characteristics of steam-water two-phase flow in a large-diameter pipe", *Nuclear Engineering and Design,* **vol. 217,** pp. 267-281. (2002)
21. J.H. Song, I.K. Park, Y.S. Shin, J.H. Kim, S.W. Hong, B.T. Min, H.D. Kim, " Fuel coolant interaction experiments in TROI using a UO2/ZrO2 mixture", *Nuclear Engineering and Design*, **222**, 1–15, (2003)